Control of glioblastoma differentiated-to-stem cell reprogramming by IRE1α/XBP1s signaling.

Dimitrios Doultsinos[1,2], Mari McMahon[1,2,3,*], Konstantinos Voutetakis[4,5,*], Joanna Obacz[1,2], Raphael Pineau[1,2], Florence Jouan[1,2], Pierre-Jean Le Reste[1,2], Akram Obiedat[6], Juhi Samal[7], John B. Patterson[8], Qingping Zheng[8], Afshin Samali[3], Abhay Pandit[7], Boaz Tirosh[6], Aristotelis Chatziioannou[4,9], Eric Chevet[1,2,10,**], Tony Avril[1,2,10,**]

[1]Proteostasis & Cancer Team, INSERM U1242 « Chemistry, Oncogenesis Stress Signaling », Université de Rennes, Rennes, France; [2]Centre Eugène Marquis, Rennes, France; [3]Apoptosis Research Centre, School of Natural Sciences, NUI Galway, Galway, Ireland; [4]Institute of Biology, Medicinal Chemistry & Biotechnology, NHRF, Athens, Greece; [5]Department of Biochemistry and Biotechnology, University of Thessaly, Larissa, Greece; [6]Institute for Drug Research, School of Pharmacy, Faculty of Medicine, Hebrew University of Jerusalem, Jerusalem, Israel; [7]CÚRAM, Centre for Research in Medical Devices, NUI Galway, Galway, Ireland; [8]Orinove Inc., Newbury Park, United States of America; [9]e-NIOS Applications PC, Kallithea-Athens, Greece; [10]Rennes Brain Cancer Team (REACT), Rennes, France.

* equal contribution

** equal contribution and corresponding authors TA (t.avril@rennes.unicancer.fr) and EC (eric.chevet@inserm.fr).

Running title: IRE1 signaling and cancer cell stemness

Keywords: Cancer stem cells, Unfolded Protein Response, Endoplasmic reticulum

Abstract

Cancer cell reprogramming contributes to antineoplastic treatment resistance and disease recurrence through cancer stem cell re-emergence. Glioblastoma multiform (GBM) is a lethal, primary, central nervous system tumor, in which reprogramming compounds prognostic severity. The endoplasmic reticulum (ER) stress sensor IRE1α (referred to as IRE1 hereafter) is a major regulator of GBM development and is identified as an appealing therapeutic target. To validate IRE1 suitability as an antineoplastic pharmacological target, we tested its involvement in GBM reprogramming. Human tumors' transcriptomic analyses showed that high IRE1 activity correlates with the down-regulation of the main stemness markers and transcription factors SOX2, SALL2, POU3F2 and OLIG2. Hence, we pharmacologically and genetically recapitulated this phenomenon in immortalized and primary GBM cell lines. Moreover, we found that IRE1/XBP1s signaling axis produces these effects through modulation of miR148a. Our results highlight a novel role of IRE1 as a negative regulator of GBM cell reprogramming and highlight opportunities of informed IRE1 modulation utility in GBM therapy.

Introduction

Glioblastoma multiforme (GBM) is the commonest primary solid tumor of the central nervous system with a dismal prognosis of median survival fewer than 2 years post diagnosis (1). GBMs are very heterogeneous differing in their resistance to chemotherapy and genetic instability (2), traits which impede therapeutic intervention, currently limited to maximal tumor resection followed by radiotherapy and chemotherapy with the alkylating agent temozolomide (3). GBM recurrence and therapeutic resistance can be attributed to cancer stem cell properties and differentiated-to-stem cell reprogramming capabilities that help GBM cells adapt to a hostile microenvironment (4). Genetic characteristics delineating tumor stem-like cells are identified with nestin and SOX2 (5); while differentiated tumor cells are usually identified with GFAP, VIM and YKL40 in the later (6).

Interestingly, nestin was shown to be overexpressed in GBM cells expressing a dominant negative form of IRE1α (hereafter called IRE1), a transducer of the Unfolded Protein Response (UPR) (7), which is an adaptive mechanism to high protein folding demand and hence misfolded protein accumulation that causes endoplasmic reticulum (ER) stress (8). IRE1 is a serine/threonine kinase and endoribonuclease, which upon ER stress oligomerizes and trans-auto phosphorylates, mediating downstream signaling events that include JNK activation, the unconventional splicing of XBP1 mRNA to produce the transcription factor XBP1s and the degradation of a specific subset of miRNAs and mRNAs; a process called RNA regulated IRE1-dependent decay or RIDD (9). GBM cells are subjected to high metabolic demand, hypoxic stress, accelerated cell cycle events and GSC (Glioblastoma Stem-like Cell) differentiation and reprogramming. To overcome these stresses, GBM cells activate partially through IRE1 signaling (10) which in turn confers tumor cells with aggressive characteristics including i) the pro-tumoral remodeling of the tumor stroma with immune and endothelial cells and ii) high migration/invasion characteristics (11). Targeting the RNase activity of IRE1 negatively impacts tumor growth due to blocking of pro-survival cellular mechanisms mediated by XBP1s. Moreover, IRE1 is involved in invasion, growth and vascularization, having been shown to carry out dual and at times antagonistic functions through XBP1s and RIDD signaling respectively, in GBM development (12, 13).

Since IRE1 and its target transcription factor XBP1s were shown to play major roles in cellular differentiation (14) and are involved in GBM development (11), we postulated that

IRE1 activity may contribute to GBM cell stemness regulation and thus we investigated the impact of IRE1 inhibition on the differentiation status of GBM cells, provided that cancer cell reprogramming contributes to antineoplastic treatment resistance and disease recurrence through cancer stem cells. Herein, we provide evidence that IRE1 negatively regulates GBM differentiated-to-stem cell reprogramming by repressing the expression of the transcription factors SOX2, SALL2, POU3F2 and OLIG2 through a novel XBP1s/miR148a signaling axis.

Results

IRE1 activity is associated with cancer differentiated state in GBM specimens

We previously identified an IRE1 activity signature of 38 genes (IRE1_38; (11, 13)) that was confronted to the TCGA GBM cohorts to stratify patients in two groups of high and low IRE1 activity. In this study we found that high IRE1 activity displayed worse prognosis compared to the cohort with low IRE1 activity (11). Since we initially observed the expression of nestin in tumors deriving from U87 cells deficient for IRE1 signaling (7), we used the IRE1_38 signature to investigate the putative IRE1 dependent expression of markers of differentiation and stemness. We found that stem cell markers were upregulated, whilst differentiation markers downregulated in tumors exhibiting low IRE1 activity as compared with those with high activity (**Figures 1A, S1A-C**). This was representative in the case of stem markers BMI1, CD133 and nestin and differentiation markers SMA, vimentin and YKL40 (**Figure 1B**). These results led us to hypothesize that IRE1 could play a causal role in cancer stem cell biology in the maintenance of the differentiation phenotype. Subsequently we tested whether IRE1 activity could impact on the expression of transcription factors (TFs) involved in GBM reprogramming. Indeed, we observed that stemness associated TFs were markedly decreased in tumors with high IRE1 activity (**Figure 1C**), the four starkest of which were OLIG2, POU3F2, SALL2 and SOX2 (**Figure 1D**). To further document this phenomenon we established whether it could be recapitulated in multiple GBM lines. To this end we utilized common available U251 and U87, as well as primary RADH87 and RADH85 (15) GBM lines genetically modified for IRE1. These cells expressed dominant negative forms of IRE1 i.e. IRE1 DN that lacks the entire cytosolic domain (13) or IRE1 Q* that is truncated at residue Q780 and lacking the RNase domain (11). We observed a marked upregulation of OLIG2, POU3F2, SALL2 and SOX2 in the IRE1 signaling deficient lines compared to parental or WT IRE1 overexpressing cells (**Figures 1E, S1F**). These data demonstrate that in tumors isolated from patients, high IRE1 activity correlates with a low expression level of reprogramming factors, which is recapitulated in both commonly available and primary GBM cell lines.

Genetic perturbation of IRE1 disturbs the differentiated phenotype of GBM cells

To further investigate the effects of IRE1 inhibition on GBM differentiated-to-stem reprogramming, we developed a culture system where cell lines normally grown in adherent

10% FCS-containing media. RADH primary cells and U87/U251 commonly available cell lines were seeded in FCS-free neurosphere culture media and cell viability, cell number, phenotype as well as the ability of cells to form spheres from single cells (clonogenicity) were determined (**Figures 2A, S2**). We observed that cells overexpressing either the DN or Q* IRE1 form readily formed spheres pertaining to a stem phenotype, this observation was lacking in parental cells or cells overexpressing IRE1 WT (**Figures 2B-C, S2A-B**). Furthermore, this was reinforced by the capacity of DN or Q* expressing cells to be grown as single cells over several passages (**Figures 2C, S2A-D**). Next, we evaluated the expression of OLIG2, POU3F2, SALL2 and SOX2 in cells grown in those conditions. Compared to parental, cells overexpressing a WT IRE1 showed no difference in the levels of any of the markers tested (**Figure 2D**). Contrastingly, cells expressing either DN or Q* IRE1 showed uniform increase of stem and reprogramming markers whilst a decrease in differentiation markers (**Figures 2D, S2E**), supporting the hypothesis that IRE1 is essential for differentiated phenotype maintenance. This was further documented at the protein level where the stemness markers SOX2, nestin and A2B5 were all upregulated whilst the differentiation marker NG2 was downregulated in IRE1 deficient cells (**Figures 2E, S2F**). Moreover, cells expressing DN or Q* IRE1 were more clonogenic compared to parental or IRE1 WT overexpressing lines (**Figures 2F, S2G**), compounding the stem phenotype in the absence of functional IRE1. Thus we concluded that in both commonly available and primary GBM cell lines, IRE1 genetic perturbation disturbs the differentiated cell phenotype, predisposing it to pre and post translational events that support a de-differentiation to a stem phenotype.

Pharmacological inhibition of IRE1 disturbs the differentiated phenotype of GBM cells

As observed for the genetic inactivation of IRE1, the use of the salicylaldehyde IRE1 ribonuclease inhibitor MKC8866 (hereafter called MKC) (16) phenocopied the effects of DN or Q* IRE1 on the capacity of cells to be grown as single cells over several passages (**Figure 3, S3**). When compared to the DMSO control, U251, RADH85, RADH87 cells treated with MKC formed spheres more readily (**Figures 3A-C, S3B-D**), displayed higher mRNA levels of stem and reprogramming markers but lower mRNA levels of differentiation markers (**Figures 3C, S3F**), as well as higher protein levels of reprogramming markers compared to differentiation markers (**Figures 3D, S3G**). The clonogenic ability of the cells was also significantly upregulated in the presence of MKC compared to control (**Figures 3E, S3H**). As such we show

that both genetic and pharmacological perturbations of IRE1 lead to a loss of differentiated phenotype and genotype whilst at the same time push cells towards a sphere stem-like phenotype, and genotype.

IRE1 signaling modestly contribute to GBM stem cell differentiation

Since IRE1 activity appears instrumental for the maintenance of the differentiated phenotype in GBM cells, we next tested whether IRE1 played a significant role in cancer stem cell differentiation. To this end, we utilized primary GBM lines grown in FCS-free neurosphere media (17) also modified for IRE1 with the Q* mutation (11), which were seeded in 10% FCS-containing media in the presence of the bone morphogenetic factor BMP4 to induce differentiation (**Figures 4A, S4A**). We first verified if the differentiation medium included FCS and BMP4 was effective in promoting differentiation of the parental RNS lines (**Figures S4B-E**). Genetic perturbation of IRE1 signaling did not result in a significant phenotype change in RNS lines when grown in FCS-containing media in the presence of BMP4 (**Figures 4B, S4B**). Moreover, the differentiation markers GFAP, O4 and TUB showed slight decreases at the mRNA level in lines overexpressing WT or Q* forms of IRE1 (**Figure 4C**), an effect recapitulated at the protein level with further significance shown between the Q* and parental, as opposed to WT and parental (**Figure 4D**). In the same line of observation, MKC treatment yielded no phenotypic changes in RNS cells in the presence of 10% FCS media and BMP4 (**Figure 4E**). Unlike what we previously observed (**Figures 2, 3**), differentiation markers show milder but still statistically significantly decrease at both the mRNA (**Figure 4F**) and protein level (**Figure 4G**). From this, we can conclude that IRE1 signaling perturbation is modestly influencing cancer stem differentiation but rather it is of paramount importance in the maintenance of the differentiated phenotype.

IRE1/XBP1s signaling maintains the differentiated state of GBM cells

It is well described that IRE1 has a dual function mediated by its ribonuclease domain (8) through either XBP1 mRNA splicing or RIDD (18). We first correlated the expression of differentiation and stem markers in tumors stratified based on their XBP1s or RIDD status. We found that tumors exhibiting high XBP1s expressed low levels of stem markers and high levels of differentiation markers (**Figure 5A**). This was confirmed by testing individual genes as well, stemness markers BMI1, CD133 and nestin showed no significant difference

between high XBP1s and high RIDD activity tumors. In the other hand, differentiated tumor cell markers SMA, vimentin and YKL40 were significantly lower in RIDD high tumors as opposed to XBP1s high tumors (**Figure 5B**). This led us to pose that XBP1s rather than RIDD is the limiting factor in maintaining the differentiated GBM cell phenotype. Next, by monitoring the expression of 15 genes involved in reprogramming in XBP1s high or RIDD high tumors, we were able to discern that reprogramming factors were downregulated in TCGA tumors with high XBP1s (**Figure 5C**). This was statistically confirmed when measuring the expression of single genes OLIG2, POU3F2, SALL2 and SOX2 (**Figure 5D**). We then sought to evaluate whether XBP1s ablation was able to recapitulate this effect in commonly available U251 and primary (RADH85 and RADH87) adherent differentiated GBM cell lines. XBP1 silencing led to the significant upregulation of almost all 4 TFs across all human lines (**Figures 5E, S5**). We thus demonstrate that it is the IRE1/XBP1s signaling axis that controls the ability of GBM cells to maintain differentiation.

XBP1s-dependent expression of miR148a prevents GBM cell reprogramming

We next sought to identify the mediating factor between XBP1s induction and reprogramming TFs downregulation and hypothesized that these factors might be miRNAs related (**Figure 6A**, (19)). Using miRNA sequencing, we first identified miRNAs whose expression is dependent on the IRE1/XBP1s signaling axis and then investigated the expression of those miRNAs in tumors stratified based on high XBP1s or high RIDD (**Figures 6B-C**). This indicated that both miR21 and miR148a were the two miRNAs presenting the highest expression in XBP1s high tumors. Interestingly, miR148a was identified previously as a transcriptional target of XBP1s using chromatin immunoprecipitation (20) and through sequence analysis we observed potential binding sites of miR148a on SOX2 **(Figures S6A-D)**. To further document the IRE1-dependent control of miR148a expression, we first showed that miR148a levels were decreased in IRE1 signaling deficient cells when comparing DN and Q* IRE1 expressing cells to their parental counterparts (**Figure 6D**). Remarkably, this also corresponded to conditions where the upregulation of SOX2 and other TFs was observed (**Figures 1-3**). To consolidate the link between the expression of miR148a and XBP1s, we next measured miR148a levels in cells silenced for XBP1s and we observed significant miR148a downregulation (**Figure 6E**). To further validate this effect *in vitro* we artificially upregulated the expression of miR148a in IRE1 deficient cells using miR148a mimics and

observed a downregulation of SOX2 as well as the majority of the other TFs as opposed to the upregulation we would normally observe (**Figures 6F, S6E**). Furthermore, to verify the link between XBP1s, miR148a and SOX2 signaling we overexpressed XBP1s in IRE1 deficient and parental cells. In these conditions we observed the subsequent upregulation of miR148a expression and the downregulation of SOX2 and other TFs in the majority of our human GBM cell lines (**Figures 6G, S6F**). A final validation of this signaling cascade was achieved by overexpressing XBP1s in IRE1 deficient cells in the presence and absence of miR148a inhibitors. As hypothesized, we observed an upregulation of XBP1s compared to untreated cells, a downregulation of miR148a and the subsequent upregulation of SOX2 (**Figure 6H**). We have thus demonstrated that reprogramming TFs including SOX2 are downregulated by miR148a, clarifying a relationship previously documented in the literature (21), and miR148a is directly induced by XBP1s (20). Therefore we provide a direct signaling cascade that governs IRE1 influence on GBM reprogramming and their ability to de-differentiate in cancer stem-like cells.

IRE1 signaling is essential for the maintenance of GBM differentiation *in vivo*

After testing our working hypothesis in cell lines and patients' tumors, we wanted to validate it and obtain more information in living tumor progression settings. To this end we measured the levels of XBP1s, miR148a and SOX2 in IRE1 knockout (KO) murine GL261 GBM cells. We found that the effect seen in human cells was recapitulated in murine GBM cells with miR148a downregulation and subsequent SOX2 upregulation following an expected XBP1s downregulation (**Figures 7A, S7**). We then proceeded to perform intracranial injections of GL261 parental or GL261 IRE1-KO cells in the brains of C57BL/6 mice. The tumor was allowed to grow and once reaching a critical mass for the mouse, the brain was harvested and multiple coronal sections were stained for the stem marker MSI1 (**Figure 7B**). Cells positive for stem marker MSI1 were quantified to discern the effect of genetic IRE1 manipulation on tumor stemness *in vivo* (**Figure 7C**). This system was also probed pharmacologically using a similar approach. Intracranial injections of GL261 parental cells formed tumors, which were allowed to grow for 14 days and then were surgically resected. A gel implant containing DMSO or MKC was subsequently placed in the tumor cavity (**Figure 7D**). The tumor was allowed to regrow and upon presentation of clinical symptoms such as

rapid weight loss, the mouse brain was removed and multiple coronal sections were stained for stem marker MSI1 to analyze its expression by immunohistochemistry (**Figure 7D**).

As is evident in the panels seen in **Figures 7B and 7E** brain sections through the tumor and the tumor periphery showed increased staining for stem marker MSI1, whilst not much difference was observed in the opposite hemisphere parenchyma. Multiple independent counts of different coronal planes for both genetic and pharmacological IRE1 inhibition quantified this effect showing a significant increase in stem marker MSI1 staining in tumors grown from GL261 IRE1-KO cells compared to those grown from GL261 parental cells (**Figure 7C**) as well as in tumors treated with MKC compared to tumors treated with DMSO (**Figure 7F**). We have thus demonstrated that IRE1 inhibition leads to an increase in the presence of stem cell markers in an *in vivo* model of GBM.

Discussion

Our comprehensive analysis of the IRE1 signaling involvement in GBM reprogramming shows the IRE1/XBP1s/miR148a axis to be a major player in the maintenance of a differentiated cancer cell phenotype and paramount in absentia to the ability of non-terminally differentiated cells to revert to a stem phenotype. Herein, we provide the first evidence of the involvement of IRE1/XBP1s signaling in the control of cancer cell reprogramming, a mechanism recently described in the acquisition of pluripotency in the reprogramming of somatic cells into stem cells (22). Moreover, we expand on an IRE1 carcinogenesis repertoire that already includes angiogenesis and metastasis, and hence further assess its suitability as an antineoplastic pharmacological target. The role of IRE1 in posttranscriptional reprogramming towards adaptation in GBM is a the subject of a plethora of studies, with mRNA and miRNA stability being the focus of some investigations (10). In particular the increase of miR17 (23) in irradiated GBM stem cells as well as its potential anti-tumoral properties (11), the decrease of tumor suppressor miR34a (24) in GBM and the increase of tumor growth promoting miR96 (25) have been documented.

The analysis of the TCGA data has indeed shed additional light on a few miRNA candidates; miR148a in particular, as especially interesting in GBM pathophysiology. Our focus on miR148a as opposed to miR21, another potential candidate our bioinformatics investigation uncovered, was guided by the demonstration that this miRNA was a transcriptional target of XBP1s (20) as well as our structural analysis of the sequence homology between miR148a and SOX2; one of the most important transcription factors in cancer cell reprogramming (**Figures S6A-D**). SOX2 and miR148a co-existed in studies examining neural crest stem cell physiology (26) and miR148a was reported as part of an investigation into the SOX2 miRNA response program in human stem cell lines (27). This of course does not exclude miR21 as a promising candidate in GBM pathophysiology. Rather, it offers further investigative scope to delve deeper in the functional network of miRNAs that may shape the response of IRE1 signaling in differentiation and reprogramming. MiR148a has been investigated in a few different malignancies with a meta-analysis showing it as a prognostic factor alongside miR148b and miR152 (28, 29). It has been shown that it promotes plasma cell differentiation by targeting germinal center TFs MITF and BACH2 (30), as well as to promote apoptosis in breast cancer cells (31). We here compound the

importance of miR148a in GBM and specifically its role in stem cell physiology and carcinogenesis in general alongside studies that have shown it to suppress the epithelial mesenchymal transition and metastasis of hepatoma cells (32), to increase glioma cell migration and invasion by downregulating GADD45A (33) and to be involved in the glabridin-induced inhibition of the cancer stem-like properties in hepatocellular carcinoma (34). We here offer an extensive investigation, and thus valuable novel information, into the relationship that miR148a has with XBP1s in the context of cancer cell reprogramming as we show that miR148a downregulates transcription factors involved in reprogramming of GBM cells upon activation by XBP1s.

It is an established fact that heterogeneity is a major barrier to successful treatment in GBM. Moreover, de-differentiation of GBM cells to a more stem-like phenotype compounds chemo-resistance. Both of these factors contribute to a basic truth of clinical trial design: it is of utmost importance to be able to stratify patients in order to maximize beneficial outcomes, as the status quo of taking broad clinical groups into consideration, has caused many a promising therapeutic candidate to fail at phase 3 clinical trials or earlier (35). We have provided so far extensive research on the involvement of IRE1 in GBM carcinogenesis (11-13, 36) and indeed patient stratification, has been a founding driver in how we have conducted this investigation. We have previously shown that using our IRE1_38 signature, tumors may be stratified according to IRE1 activity (high IRE1 activity conferring worse prognosis) as well as according to the XBP1s or RIDD activity (XBP1s conferring worse prognosis) (11). Here we provide evidence that IRE1 inhibition and particularly XBP1s inhibition might promote differentiated tumor cells to revert to a more stem-like phenotype, an effect that has been linked with chemo-resistance and oncogenesis in general in GBM (37).

As such our results point to two distinct opportunities for utilizing IRE1 signaling as therapeutic target in GBM. Firstly, patients with XBP1s low expressing tumors could benefit from IRE1 inhibition as GBM cells would have little capacity to utilize this signaling pathway for reverting to a stem phenotype and UPR disruption would overload a stress response mechanism that would already have to deal with a hostile microenvironment or with treatment. Indeed a recent study has shown that the IRE1/XBP1s axis is important in the adaptation to stress of leukaemic and healthy haematopoietic stem cells, as they enhance the ability of these cells to overcome ER stress and survive, promoting carcinogenesis (38).

This information compounds the second and potentially more important outcome of our study that shows the attractiveness of IRE1 targeting therapeutics as adjuvant therapy alongside the currently established trident of surgery, chemotherapy and radiotherapy in GBM. The rationale would be that IRE1 targeting can sensitize GBM cells to therapy as it would weaken their responses and disallow them the time to adapt to the hostile conditions afforded by chemotherapy. As such patients would benefit by not only potential drops in the rates of tumor re-emergence but also of reduced need for repeated therapy doses, which by default carry unfavorable toxicity profiles.

In conclusion, having demonstrated the importance of IRE1 in GBM development, prognosis and aggressiveness and having reviewed the role that GSCs play in similar characteristics we investigated the link between IRE1 signaling and GBM capacity in differentiation and reprogramming and sought to build upon the functionality of IRE1 in GBM pathophysiology. We described i) a direct link of IRE1 signaling to differentiated cells reprogramming to stem cells in cell culture and mouse models and ii) the correlation between low IRE1 activity and the enrichment in cancer cell markers in patients tumors. Thereafter we delved further into the mechanisms of this IRE1 control and propose a novel concept where inhibition of XBP1s signaling induces the expression of transcription factors involved in GBM reprogramming and showcase the downstream miR148a signaling that makes this possible. Our work not only adds to the repertoire of IRE1 activity in GBM but also offers scope for patients' stratification and combination therapy development with IRE1 targeting at its epicenter. It achieves this whilst reinforcing the need for strict pharmacovigilance when considering the risks of novel therapeutic design and builds upon our previous work in the field of translational neuro-oncology and ER biology to provide an ever more detailed landscape of IRE1 involvement and thus scrutinize the exploitability of the modulation of its function.

Materials & Methods

Reagents and antibodies

All reagents not specified below were purchased from Sigma-Aldrich (St Quentin Fallavier, France). Recombinant human BMP4 protein was obtained from R&D Systems (Lille, France); MKC8866 from Fosun Orinove (Suzhou, China); siRNA targeting XBP1, miR148a inhibitors, mimics and controls (miRvana) were purchased from Thermo Fisher Scientific (Montigny le Bretonne, France). For flow cytometry, antibodies against human NG2, nestin, O4, SOX2, and TUB were obtained from R&D Systems, Biotechne (Lille, France); anti-A2B5 from Miltenyi Biotec (Paris, France); anti- GFAP from eBioscience (Thermo Fisher Scientific), anti-MSI1 from Chemicon (Merck Millipore, Molsheim, France) (**Table S1**).

Cell culture and treatments

U87MG (ATCC) and U251MG (Sigma, St Louis, MO, USA) cells were authenticated as recommended by AACR (http://aacrjournals.org/content/cell-line-authentication-information) and tested for the absence of mycoplasma using MycoAlert® (Lonza, Basel, Switzerland) or MycoFluor (Invitrogen, Carlsbad, CA, USA). Primary GBM cell lines were obtained as described in (17). U87, U251 and primary RADH GBM cells were grown in DMEM Glutamax (Invitrogen, Carlsbad, CA, USA) supplemented with 10% FBS. Primary GBM stem-like cell lines (RNS) were grown in DMEM/Ham's:F12 (Life Technologies) supplemented with B27 and N2 additives (Life Technologies), EGF (20 ng/ml) and basic FGF (20 ng/ml) (Peprotech, Neuilly-sur Seine, France). Primary RADH85, RADH87, RNS85 and RNS87 were stably transfected at MOI = 0.3 with pCDH-CMV-MCS-EF1-Puro-copGFP (System biosciences) empty vector (EV), pCDH-CMV-MCS-EF1-Puro-copGFP containing IRE1α wild-type sequence (WT), or mutated sequence (Q780*). These cells were selected using 2 µg/ml puromycin, and polyclonal populations were tested for GFP expression. Transfections of GBM primary cell lines with IRE1 WT and Q780* were performed using Lipofectamine LTX (Thermo Fisher Scientific), according to the manufacturer's instructions. Murine GBM GL261 IRE1 KO was generated as described in (39) using specific sgRNAs to the mouse IRE1 (Fwd#1: 5'-CACCGCAGGGTCGAGACAAACAACA-3' and Rev#1: 5'-AAACTGTTGTTTGTCTCGACCCTGC-3'; Fwd#2: 5'-CACCGCAAAATAGGTGGCATTCCAG-3' and Rev#2: 5'-AAACCTGGAATGCCACCTATTTTGC-3'. GL261 cells were grown in DMEM Glutamax

supplemented with 10% FBS. For XBP1s overexpression, cells were transiently transfected for 48 hours with XBP1s plasmid (Addgene, Teddington, United Kingdom) using Lipofectamine 2000 (Thermo Fisher Scientific), according to the manufacturer's instructions. For siRNA XBP1s experiments, cells were transiently transfected for 48 hours with control and siRNA targeting XBP1s (Eurofins Genomics, Les Ulis, France, 5' AGAAGGCUCGAAUGAGUG 3') using Lipofectamine iRNA max (Thermo Fisher Scientific), according to the manufacturer's instructions. For miR148a treatment, cells were transiently transfected for 48 hours with miR148a mimics or inhibitors (miRvana) using Lipofectamine iRNA max (Thermo Fisher Scientific), according to the manufacturer's instructions.

Patients' transcriptomic data from TCGA

The publicly available GBM dataset of The Cancer Genome Atlas (TCGA) (Consortium et al., 2007; consortium, 2008) was assessed from the NCBI website platform (https://gdc-portal.nci.nih.gov) and was analyzed using the BioInfominer (40) analysis pipeline (E-Nios, Greece, https://bioinfominer.com), which performs statistical, semantic network, topological analysis, exploiting various biological hierarchical vocabularies, with the aim to unearth, detect and rank significantly altered biological processes and the respective driver genes linking these processes. Genes were considered significantly differentially expressed if the p value was below 0.05. To analyze the miRNA database, hierarchical clustering algorithms and Pearson correlation analyses were carried out using R packages.

Quantitative real-time PCR

Total RNA was prepared using the TRIzol reagent (Invitrogen, Carlsbad, CA, USA). Semi-quantitative analyses were carried out as previously described (12, 13) (12,16). All RNAs were reverse-transcribed with Maxima Reverse Transcriptase (Thermo Scientific), according to manufacturer protocol. qPCR was performed with a StepOnePlus™ Real-Time PCR Systems from Applied Biosystems and the SYBR Green PCR Core reagents kit (Takara, Ozyme, Saint Cyr L'Ecole, France). All RNAs for the miRNA investigation were transcribed using miScript RT kits and subsequent qPCR performed using miScript Primer Assays and miScript SYBR kits (Qiagen, Courtaboeuf). Experiments were performed with at least triplicates for each data point. Each sample was normalized on the basis of its expression of the *actin* gene. For quantitative PCR, the primer pairs used are described in **Table S2**.

Mouse Intracranial injections

Eight-week old male C57BL/6 mice were housed in an animal care unit authorized by the French Ministries of Agriculture and Research (Biosit, Rennes, France - Agreement No. B35-238-40). All animal procedures met the European Community Directive guidelines (DIR MESR 13480) and were approved by the local ethics committee No. 007. The protocol used was as previously described (7). Cell implantations were at 2 mm lateral to the bregma and 3 mm in depth using GL261 cells. Mice were daily clinically monitored and sacrificed at first clinical signs. In the experiments with MKC plug, fourteen days post-injection, the tumor formed was maximally removed without killing the animal and a plug infused with MKC or DMSO control was implanted in the resection cavity. At first clinical signs, mouse brains were collected, fixed in 4% formaldehyde solution and paraffin embedded for histological analysis using anti-vimentin antibody (Interchim, Montluçon, France) to visualize the tumor masses.

Immunohistochemistry analyses

Mouse tumor tissues were fixed in 4% neutral buffered formalin, embedded in paraffin, cut into 5-µm thick sections and mounted on slides. The immunohistochemistry (IHC) labeling were carried out using the H2P2 imaging platform of the faculty of Rennes. For cancer stem cell immunodetection, the sections were incubated 1 hour at room temperature with anti-MSI1 antibody (1:500 dilution; Merk Millipore). Immunostaining was carried out using the BenchMark XT (Ventana Medical Systems, Illkirch Graffenstaden, France) with the OmniMap kit (a “biotin-free” system using multimer technology, Roche, Boulogne Billancourt, France) and a Tris borate EDTA pH8 buffer for antigen retrieval. Sections were analyzed with an Axioplan 2 epifluorescent microscope (Zeiss, Marly-le-Roi, France) equipped with a digital camera Axiocam (Zeiss), and were converted on to digital slides with the scanner Nanozoomer 2.0-RS (Hamamatsu, Meyer Instruments, Houston, United-States of America). ImmunoRatio, the publicly available web application (http://153.1.200.58:8080/immunoratio/) for automated image analysis, was used to determine the number of MSI1-stained cells.

Flow cytometry analyses

Cells were washed in PBS 2% FBS and incubated with saturating concentrations of human immunoglobulins and fluorescent-labelled primary antibodies for 30 min at 4°C. Cells were then washed with PBS 2% FBS and analyzed by flow cytometry using a NovoCyte NovoSampler Pro (ACEA Biosciences, Ozyme). The population of interest was gated according to its FSC/SSC criteria. Data were analyzed with the NovoExpress software (ACEA Biosciences). For intracellular staining, cells were permeabilized using BD Cytofix/Cytoperm and BD Perm/Wash reagents (BD Biosciences, Le Pont de Claix, France) according to the manufacturer's instructions. Protein expression levels were given by the ration of mean of fluorescence obtained with the antibody of interest divided by the mean of fluorescence obtained with the isotype control (rMFI).

Statistical analyses

Data are presented as mean ± SD or SEM (as indicated). Statistical significance ($P < 0.05$ or less) was determined using a paired or unpaired t-test or ANOVA as appropriate and performed using GraphPad Prism software (GraphPad Software, San Diego, CA, USA).

Acknowledgements

We thank the Biosit histopathology H2P2 platform (Université de Rennes 1, France) for immunohistochemistry analyses on tumor xenografts; and the Biosit ARCHE animal facility (Université de Rennes 1) for animal housing. This work was funded by grants from Institut National du Cancer (INCa PLBIO), Fondation pour la Recherche Médicale (FRM, équipe labellisée 2018) to EC; EU H2020 MSCA ITN-675448 (TRAINERS) and MSCA RISE-734749 (INSPIRED) grants to AS, EC, EC; PHC Maimonide 2017-2018 to BT and EC; the David R. Bloom Center for Pharmacy, the Dr. Adolph and Klara Brettler Center for Research in Pharmacology, German Israeli Fund (grant no. I-1471-414.13/2018) to BT; PROMISE, 12CHN 204 Bilateral Greece-China Research Program of the Hellenic General Secretariat of Research and Technology and the Chinese Ministry of Research and Technology sponsored by the Program "Competitiveness and Entrepreneurship," Priority Health of the Peripheral Entrepreneurial Program of Attiki to AC. DD is a Marie Curie early stage researcher funded by EU H2020 MSCA ITN-675448 (TRAINERS). JO was funded by a post-doctoral fellowship from "Région Bretagne". JS is funded by Hardiman Fellowship and Science Foundation Ireland (SFI) and the European Regional Development Fund (Grant Number 13/RC/2073). MMM was funded by the Irish Research Council and an ARED International PhD fellowship from "Région Bretagne".

Author contribution

DD – conceptualization, methodology, investigation; **MM, JO, RP, FJ, PJLR, AO, JS, AP, BT –** methodology, investigation; **KV –** data curation, formal analysis; **AC –** data curation, formal analysis funding acquisition; **JBP, QZ –** resources; **AS, BT –** resources, funding acquisition; **EC –** supervision, conceptualization, project administration, funding acquisition; writing; **TA –** supervision, conceptualization, methodology, investigation, project administration, writing (https://www.casrai.org/credit.html#)

Conflict of interest

EC and AS are founders of Cell Stress Discoveries Ltd (https://cellstressdiscoveries.com/). AC is the founder of e-NIOS Applications PC (https://e-nios.com/).

References

1. Ellis HP, Greenslade M, Powell B, Spiteri I, Sottoriva A, Kurian KM. Current Challenges in Glioblastoma: Intratumour Heterogeneity, Residual Disease, and Models to Predict Disease Recurrence. Frontiers in oncology. 2015;5:251.
2. Shapiro JR, Yung W-KA, Shapiro WR. Isolation, Karyotype, and Clonal Growth of Heterogeneous Subpopulations of Human Malignant Gliomas. Cancer research. 1981;41(6):2349 LP - 59.
3. Stupp R, Mason WP, van den Bent MJ, Weller M, Fisher B, Taphoorn MJBB, et al. Radiotherapy plus concomitant and adjuvant temozolomide for glioblastoma. The New England journal of medicine. 2005;352(10):987-96.
4. Hu B, Wang Q, Wang YA, Hua S, Sauvé C-EG, Ong D, et al. Epigenetic Activation of WNT5A Drives Glioblastoma Stem Cell Differentiation and Invasive Growth. Cell. 2016;167(5):1281-95.e18.
5. Neradil J, Veselska R. Nestin as a marker of cancer stem cells. Cancer science. 2015;106(7):803-11.
6. Widestrand Å, Faijerson J, Wilhelmsson U, Smith PLP, Li L, Sihlbom C, et al. Increased Neurogenesis and Astrogenesis from Neural Progenitor Cells Grafted in the Hippocampus of GFAP−/−Vim−/− Mice. STEM CELLS. 2007;25(10):2619-27.
7. Auf G, Jabouille A, Guérit S, Pineau R, Delugin M, Bouchecareilh M, et al. Inositol-requiring enzyme 1alpha is a key regulator of angiogenesis and invasion in malignant glioma. Proceedings of the National Academy of Sciences of the United States of America. 2010;107(35):15553-8.
8. Doultsinos D, Avril T, Lhomond S, Dejeans N, Guédat P, Chevet E. Control of the Unfolded Protein Response in Health and Disease. SLAS DISCOVERY: Advancing Life Sciences R&D. 2017;22(7):2472555217701685.
9. Almanza A, Carlesso A, Chintha C, Creedican S, Doultsinos D, Leuzzi B, et al. Endoplasmic reticulum stress signalling – from basic mechanisms to clinical applications. The FEBS journal. 2018;0(0).
10. Obacz J, Avril T, Le Reste P-J, Urra H, Quillien V, Hetz C, et al. Endoplasmic reticulum proteostasis in glioblastoma—From molecular mechanisms to therapeutic perspectives. Science signaling. 2017;10(470).
11. Lhomond S, Avril T, Dejeans N, Voutetakis K, Doultsinos D, McMahon M, et al. Dual IRE1 RNase functions dictate glioblastoma development. EMBO molecular medicine. 2018;10(2):139-308.
12. Dejeans N, Pluquet O, Lhomond S, Grise F, Bouchecareilh M, Juin A, et al. Autocrine control of glioma cells adhesion and migration through IRE1alpha-mediated cleavage of SPARC mRNA. Journal of cell science. 2012;125(Pt 18):4278-87.
13. Pluquet O, Dejeans N, Bouchecareilh M, Lhomond S, Pineau R, Higa A, et al. Posttranscriptional regulation of per1 underlies the oncogenic function of IRE?? Cancer research. 2013;73(15):4732-43.
14. Bettigole S, Lis R, Adoro S, Lee AH, Spencer LA, Weller PF, et al. The transcription factor XBP1 is selectively required for eosinophil differentiation. Nature Immunology. 2015;16(8):829-37.
15. Avril T, Etcheverry A, Pineau R, Obacz J, Jegou G, Jouan F, et al. CD90 Expression Controls Migration and Predicts Dasatinib Response in Glioblastoma. Clinical Cancer Research. 2017;23(23):7360 LP - 74.

16. Volkmann K, Lucas JL, Vuga D, Wang X, Brumm D, Stiles C, et al. Potent and selective inhibitors of the inositol-requiring enzyme 1 endoribonuclease. The Journal of biological chemistry. 2011;286(14):12743-55.
17. Avril T, Vauleon E, Hamlat A, Saikali S, Etcheverry A, Delmas C, et al. Human Glioblastoma Stem-Like Cells are More Sensitive to Allogeneic NK and T Cell-Mediated Killing Compared with Serum-Cultured Glioblastoma Cells. Brain pathology. 2012;22(2):159-74.
18. Maurel M, Chevet E, Tavernier J, Gerlo S. Getting RIDD of RNA: IRE1 in cell fate regulation. Trends in biochemical sciences. 2014;39(5):245-54.
19. McMahon M, Samali A, Chevet E. Regulation of the unfolded protein response by noncoding RNA. American Journal of Physiology-Cell Physiology. 2017;313(3):C243-C54.
20. Cho YM, Kim T-M, Hun Kim D, Hee Kim D, Jeong S-W, Kwon O-J. miR-148a is a downstream effector of X-box-binding protein 1 that silences Wnt10b during adipogenesis of 3T3-L1 cells. Experimental &Amp; Molecular Medicine. 2016;48:e226.
21. Lopez-Bertoni H, Lal B, Li A, Caplan M, Guerrero-Cázares H, Eberhart CG, et al. DNMT-dependent suppression of microRNA regulates the induction of GBM tumor-propagating phenotype by Oct4 and Sox2. Oncogene. 2015;34(30):3994-4004.
22. Simic MS, Moehle EA, Schinzel RT, Lorbeer FK, Halloran JJ, Heydari K, et al. Transient activation of the UPR(ER) is an essential step in the acquisition of pluripotency during reprogramming. Sci Adv. 2019;5(4):eaaw0025.
23. Li H, Yang BB. Stress response of glioblastoma cells mediated by miR-17-5p targeting PTEN and the passenger strand miR-17-3p targeting MDM2. Oncotarget. 2013;3(12):1653-68.
24. Li Y, Guessous F, Zhang Y, Dipierro C, Kefas B, Johnson E, et al. MicroRNA-34a inhibits glioblastoma growth by targeting multiple oncogenes. Cancer research. 2009;69(19):7569-76.
25. Yan Z, Wang J, Wang C, Jiao Y, Qi W, Che S. miR-96/HBP1/Wnt/β-catenin regulatory circuitry promotes glioma growth. FEBS letters. 2014;588(17):3038-46.
26. Ichi S, Costa FF, Bischof JM, Nakazaki H, Shen Y-W, Boshnjaku V, et al. Folic acid remodels chromatin on Hes1 and Neurog2 promoters during caudal neural tube development. The Journal of biological chemistry. 2010;285(47):36922-32.
27. Vencken SF, Sethupathy P, Blackshields G, Spillane C, Elbaruni S, Sheils O, et al. An integrated analysis of the SOX2 microRNA response program in human pluripotent and nullipotent stem cell lines. BMC genomics. 2014;15:711.
28. Miao C, Zhang J, Zhao K, Liang C, Xu A, Zhu J, et al. The significance of microRNA-148/152 family as a prognostic factor in multiple human malignancies: a meta-analysis. Oncotarget. 2017;8(26):43344-55.
29. Friedrich M, Pracht K, Mashreghi M-F, Jäck H-M, Radbruch A, Seliger B. The role of the miR-148/-152 family in physiology and disease. European journal of immunology. 2017;47(12):2026-38.
30. Porstner M, Winkelmann R, Daum P, Schmid J, Pracht K, Côrte-Real J, et al. miR-148a promotes plasma cell differentiation and targets the germinal center transcription factors Mitf and Bach2. European journal of immunology. 2015;45(4):1206-15.
31. Li Q, Ren P, Shi P, Chen Y, Xiang F, Zhang L, et al. MicroRNA-148a promotes apoptosis and suppresses growth of breast cancer cells by targeting B-cell lymphoma 2. Anti-cancer drugs. 2017;28(6).

32. Zhang JP, Zeng C, Xu L, Gong J, Fang JH, Zhuang SM. MicroRNA-148a suppresses the epithelial–mesenchymal transition and metastasis of hepatoma cells by targeting Met/Snail signaling. Oncogene. 2013;33:4069.
33. Cui D, Sajan P, Shi J, Shen Y, Wang K, Deng X, et al. MiR-148a increases glioma cell migration and invasion by downregulating GADD45A in human gliomas with IDH1 R132H mutations. Oncotarget. 2017;8(15):25345-61.
34. Jiang F, Mu J, Wang X, Ye X, Si L, Ning S, et al. The Repressive Effect of miR-148a on TGF beta-SMADs Signal Pathway Is Involved in the Glabridin-Induced Inhibition of the Cancer Stem Cells-Like Properties in Hepatocellular Carcinoma Cells. PloS one. 2014;9(5):e96698.
35. von Neubeck C, Seidlitz A, Kitzler HH, Beuthien-Baumann B, Krause M. Glioblastoma multiforme: emerging treatments and stratification markers beyond new drugs. The British journal of radiology. 2015;88(1053):20150354.
36. Lhomond S, Pallares N, Barroso K, Schmit K, Dejeans N, Fazli H, et al. Adaptation of the secretory pathway in cancer through IRE1 signaling. Methods in molecular biology. 2015;1292:177-94.
37. Gargiulo G, Cesaroni M, Serresi M, de Vries N, Hulsman D, Bruggeman Sophia W, et al. In Vivo RNAi Screen for BMI1 Targets Identifies TGF-β/BMP-ER Stress Pathways as Key Regulators of Neural- and Malignant Glioma-Stem Cell Homeostasis. Cancer cell. 2013;23(5):660-76.
38. Liu L, Zhao M, Jin X, Ney G, Yang KB, Peng F, et al. Adaptive endoplasmic reticulum stress signalling via IRE1α–XBP1 preserves self-renewal of haematopoietic and pre-leukaemic stem cells. Nature cell biology. 2019;21(3):328-37.
39. Obiedat A, Seidel E, Mahameed M, Berhani O, Tsukerman P, Voutetakis K, et al. Transcription of the NKG2D ligand MICA is suppressed by the IRE1/XBP1 pathway of the unfolded protein response through the regulation of E2F1. FASEB journal : official publication of the Federation of American Societies for Experimental Biology. 2019;33(3):3481-95.
40. Georgiadis P, Liampa I, Hebels DG, Krauskopf J, Chatziioannou A, Valavanis I, et al. Evolving DNA methylation and gene expression markers of B-cell chronic lymphocytic leukemia are present in pre-diagnostic blood samples more than 10 years prior to diagnosis. BMC genomics. 2017;18(1):728.

Figure Legends

Figure 1. **IRE1 activity is associated with cancer differentiated state in GBM specimens. A)** Hierarchical clustering of GBM patients (TCGA cohort) based on high or low IRE1 activity confronted to differentiation and stem gene signatures derived from literature. **B)** mRNA expression of BMI1, CD133, nestin stem cell markers and SMA, vimentin, YKL40 differentiated cell markers based on microarray fluorescence intensity in high and low IRE1 activity tumors (TCGA cohort). **C)** Hierarchical clustering of GBM patients (TCGA cohort) based on high or low IRE1 activity confronted to a reprogramming TFs signature derived from literature. **D)** mRNA levels of reprogramming TFs OLIG2, POU3F2, SALL2, and SOX2 based on microarray fluorescence intensity in high and low IRE1 activity tumors (TCGA cohort). **E)** mRNA levels of reprogramming TFs in U251, RADH85 and RADH87 lines expressing WT, DN or Q* forms of IRE1 normalized to parental. (ns): not significant; (*): $p<0.05$; (**): $p<0.01$; (***): $p<0.001$.

Figure 2. **Genetic perturbation of IRE1 effect on GBM cell reprogramming. A)** Schematic representation of GBM cell working model of differentiated to stem cell phenotype culture. **B)** Phenotypic characterization of U251/ RADH85/ RADH87 parental and overexpressing WT, DN or Q* forms of IRE1 when grown in neurosphere media. **C)** Differentiated GBM cell lines U251, RADH85 and RADH87 were cultured in neurosphere medium and were passaged every 14 days. If the number of cells was under the initial number of cells seeded (10^6), the culture was stopped (n=2 to 4). **D)** Heat map representation of fold change of mRNA expression of genes involved in reprogramming, stemness and differentiation normalized to parental in U251, RADH85, RADH87 lines expressing WT, DN or Q* forms of IRE1 when grown in neurosphere media. **E)** Protein expression of reprogramming, stemness and differentiation markers in these lines compared to parental lines determined by flow cytometry. **F)** Clonogenicity of differentiated lines expressing WT, DN or Q* forms of IRE1 compared to parental lines when grown in neurosphere media. (ns): not significant; (*): $p<0.05$; (**): $p<0.01$; (***): $p<0.001$.

Figure 3. Pharmacological inhibition of IRE1 effect on GBM cell reprogramming. A) Differentiated GBM cell lines U251, RADH85 and RADH87 were cultured in neurosphere

medium in the presence of MKC (5 µM), and were passaged every 14 days. If the number of cells was under the initial number of cells seeded (10^6), the culture is stopped (n=2 to 3). **B)** Phenotypic characterization of parental adherent (RADH85/87 and U251) lines through culture in neurosphere medium treated with MKC or DMSO. **C)** Heat map representation of fold change of mRNA expression of genes involved in reprogramming, stemness and differentiation normalized to parental in U251, RADH85, and RADH87 lines when grown in neurosphere media in the presence of MKC or DMSO. **D)** Protein expression of reprogramming, stemness and differentiation markers in these lines compared to parental lines determined by flow cytometry. **E)** Quantification of clonogenicity of single cell parental, WT or Q* IRE1 expressing RADH85/87 and U251 lines when seeded in serum-free medium in the presence of MKC or DMSO. (ns): not significant; (*): p<0.05; (**): p<0.01; (***): p<0.001.

Figure 4. Role of IRE1 in GBM stem-to-differentiated state reprogramming. A) Schematic representation of GBM cell working model of stem-to-differentiated cell phenotype culture. **B)** Phenotypic characterization of RNS85/87 parental and overexpressing WT or Q* forms of IRE1 when grown in FCS and BMP4 containing media. **C)** Heat map representation of fold change of mRNA expression of genes involved in differentiation normalized to parental in RNS85, RNS87 lines expressing WT or Q* forms of IRE1 when grown in FCS and BMP4 containing media. **D)** Protein expression of differentiation markers in these lines normalized to parental determined by flow cytometry. **E)** Phenotypic characterization of parental RNS85/87 lines through culture in FCS and BMP4 containing medium treated with MKC or DMSO. **F)** Heat map representation of fold change of mRNA expression of genes involved in differentiation in parental RNS85, RNS87 lines when grown in FCS and BMP4 containing media in the presence of MKC or DMSO. **G)** Protein expression of differentiation markers in these lines in the presence of MKC or DMSO determined by flow cytometry. (ns): not significant; (*): p<0.05; (**): p<0.01; (***): p<0.001.

Figure 5. XBP1s involvement in GBM cell reprogramming. A) Hierarchical clustering of genes involved in differentiation and stemness in GBM (TCGA cohort) based on high XBP1s or high RIDD activity (blue low levels, red high levels). **B)** mRNA expression of BMI1, CD133, nestin stem cell markers and SMA, vimentin, YKL40 differentiated cell markers based on microarray fluorescence intensity in high XBP1s and high RIDD activity tumors (TCGA cohort). **C)**

Hierarchical clustering of genes involved in reprogramming in GBM (TCGA cohort) based on high XBP1s or high RIDD activity (blue low levels, red high levels). **D)** mRNA expression of SOX2, POU3F2, OLIG2, SALL2 reprogramming TFs based on microarray fluorescence intensity in high XBP1s and high RIDD activity tumors (TCGA cohort). **E)** mRNA levels of SOX2 upon XBP1s silencing in primary and classical adherent GBM lines (RADH85/87 and U251 respectively). (ns): not significant; (*): p<0.05; (**): p<0.01; (***): p<0.001.

Figure 6. XBP1s-dependent expression of miR148a prevents GBM cell reprogramming. A) Schematic representation of hypothesis of effect of IRE1 signaling on reprogramming TFs. **B)** Hierarchical clustering of miRNAs in GBM (TCGA cohort) confronted to high XBP1s or high RIDD activity (blue low levels, red high levels) with the best 5 candidates shown. **C)** mRNA expression of miR148a based on microarray fluorescence intensity in high XBP1s and high RIDD activity tumors (TCGA cohort). **D)** miR148a expression in adherent lines U251, RADH85/87 expressing DN or Q* forms of IRE1 normalized to parental. **E)** miR148a expression in adherent lines U251, RADH85/87 transiently deficient for XBP1s through siRNA transfection compared to control. **F)** SOX2 and miR148a expression levels in RADH85 IRE1 Q* expressing cells in the presence of miR148a mimic compared to control. **G)** XBP1s, SOX2 and miR148a expression levels in RADH85 IRE1 Q* expressing cells, over-expressing XBP1s compared to control. **H)** XBP1s, SOX2 and miR148a expression levels in RADH85 IRE1 Q* expressing cells, over-expressing XBP1s, in the presence of miR148a inhibitors compared to control. (ns): not significant; (*): p<0.05; (**): p<0.01; (***): p<0.001.

Figure 7. IRE1-dependent control of GBM stemness reprogramming *in vivo*. A) XBP1s, SOX2 and miR148a expression levels in GL261 IRE1 KO cells, compared to parental. **B)** Representative sections of tumors grown from GL261 parental or GL261 IRE1-KO cells injected in the brain of orthotopic syngeneic mouse model, stained for MSI. Sections from tumor body, tumor periphery and opposite to tumor brain parenchyma shown. **C)** Quantification of MSI1 positive cells (3-4 tumors/condition, 10 random fields/tumor/condition quantified, two independent counts). **D)** Orthotopic syngeneic mouse GBM model and peri-operative treatment with MKC (plug). **E)** MSI1 staining (stem marker) of tumor body or periphery and opposite to tumor site hemisphere parenchyma. This was performed in GL261 derived tumors treated with control or MKC plugs. **F)** Quantification of

MSI1 positive cells (3 tumors/condition, 10 random fields/tumor/condition quantified, three independent counts). (ns): not significant; (*): p<0.05; (**): p<0.01; (***): p<0.001.

FIGURE 1

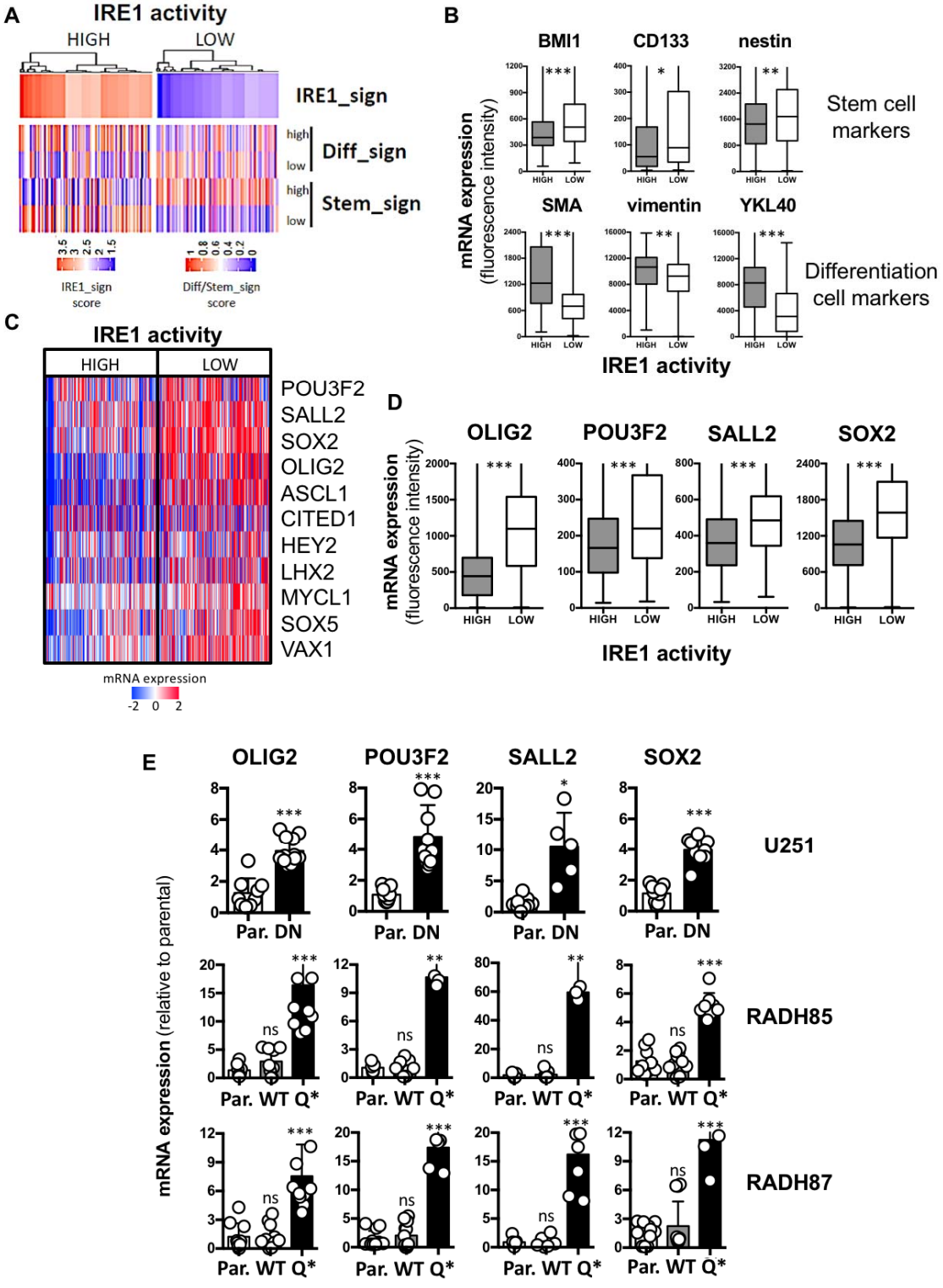

FIGURE 2

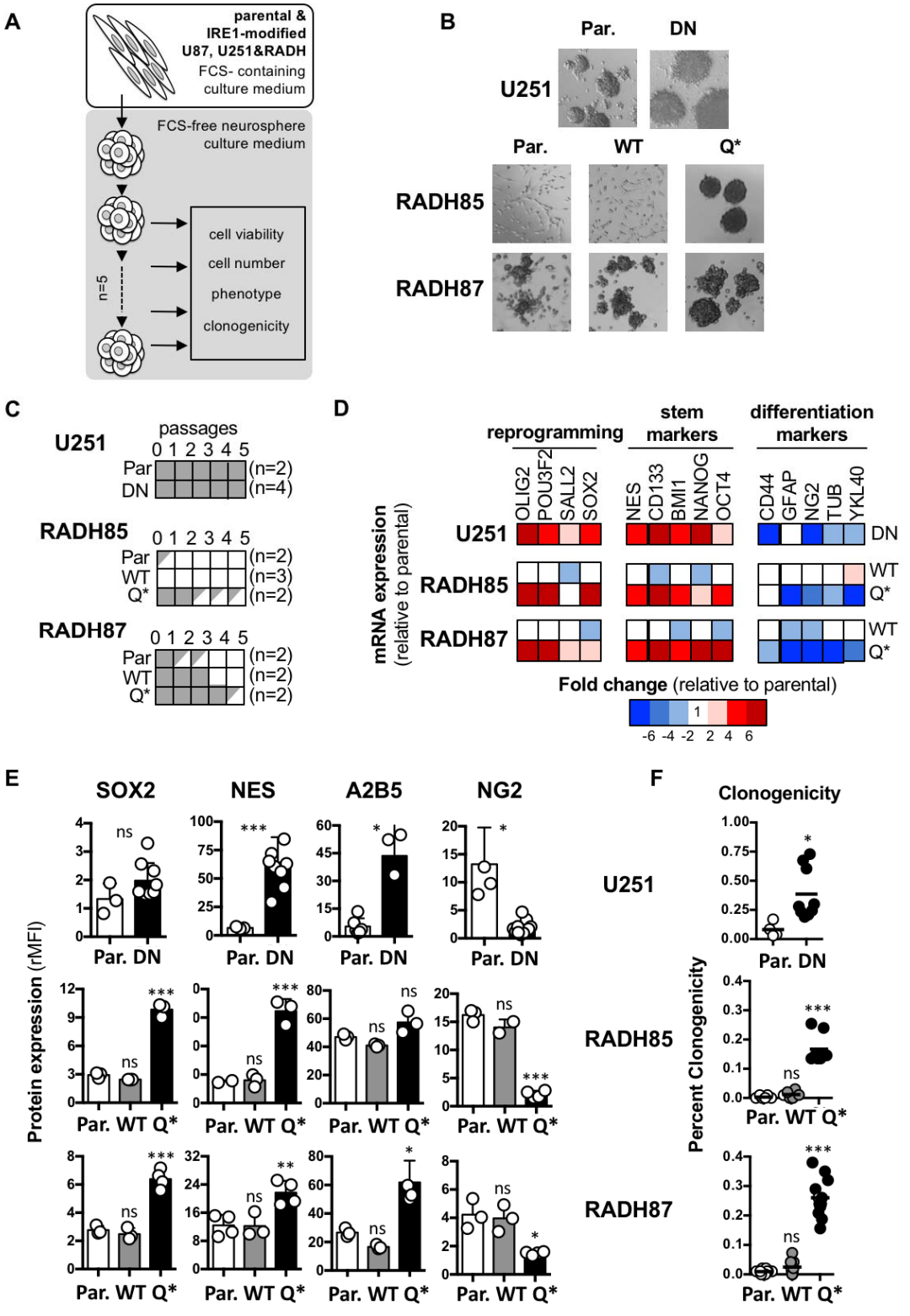

FIGURE 3

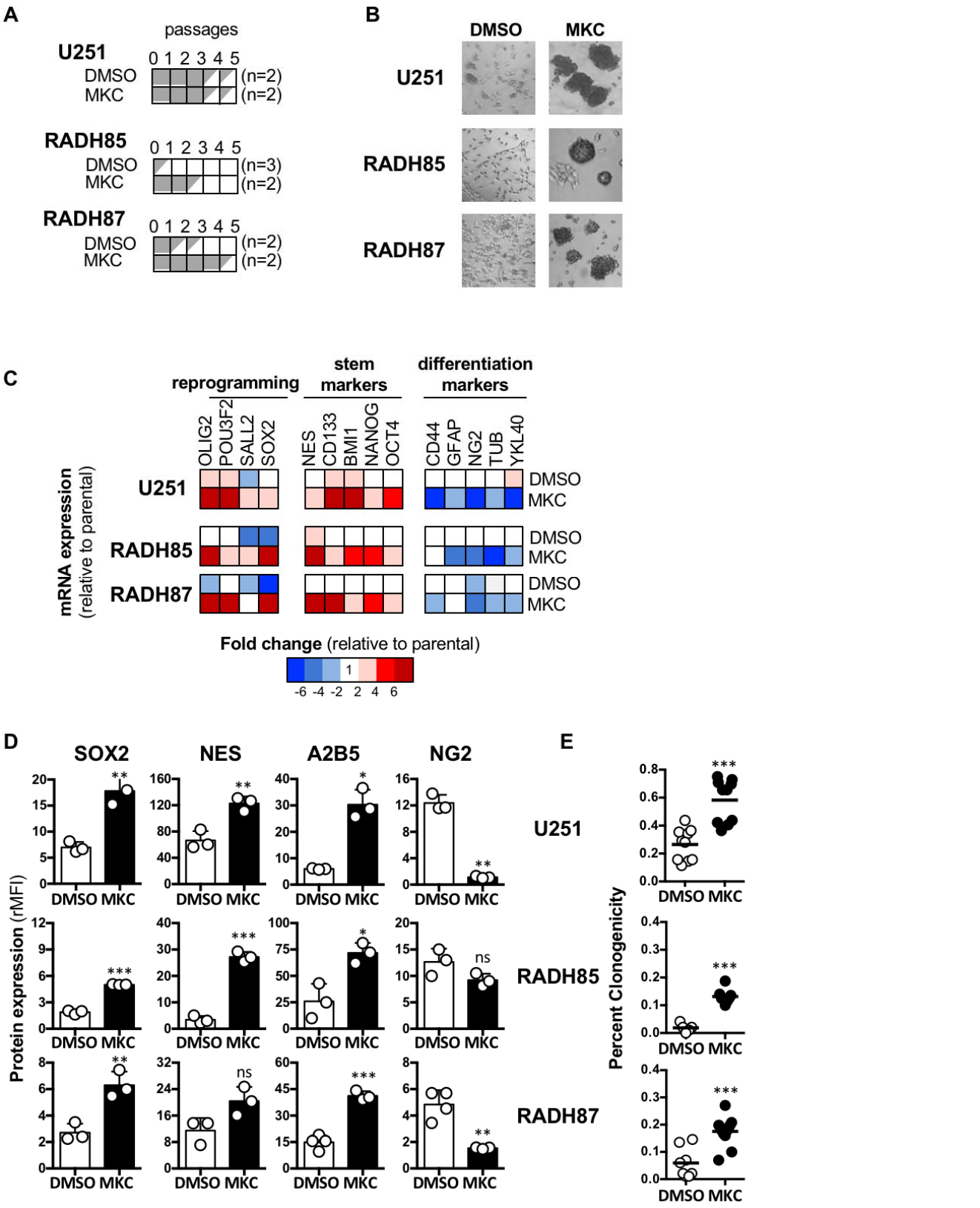

FIGURE 4

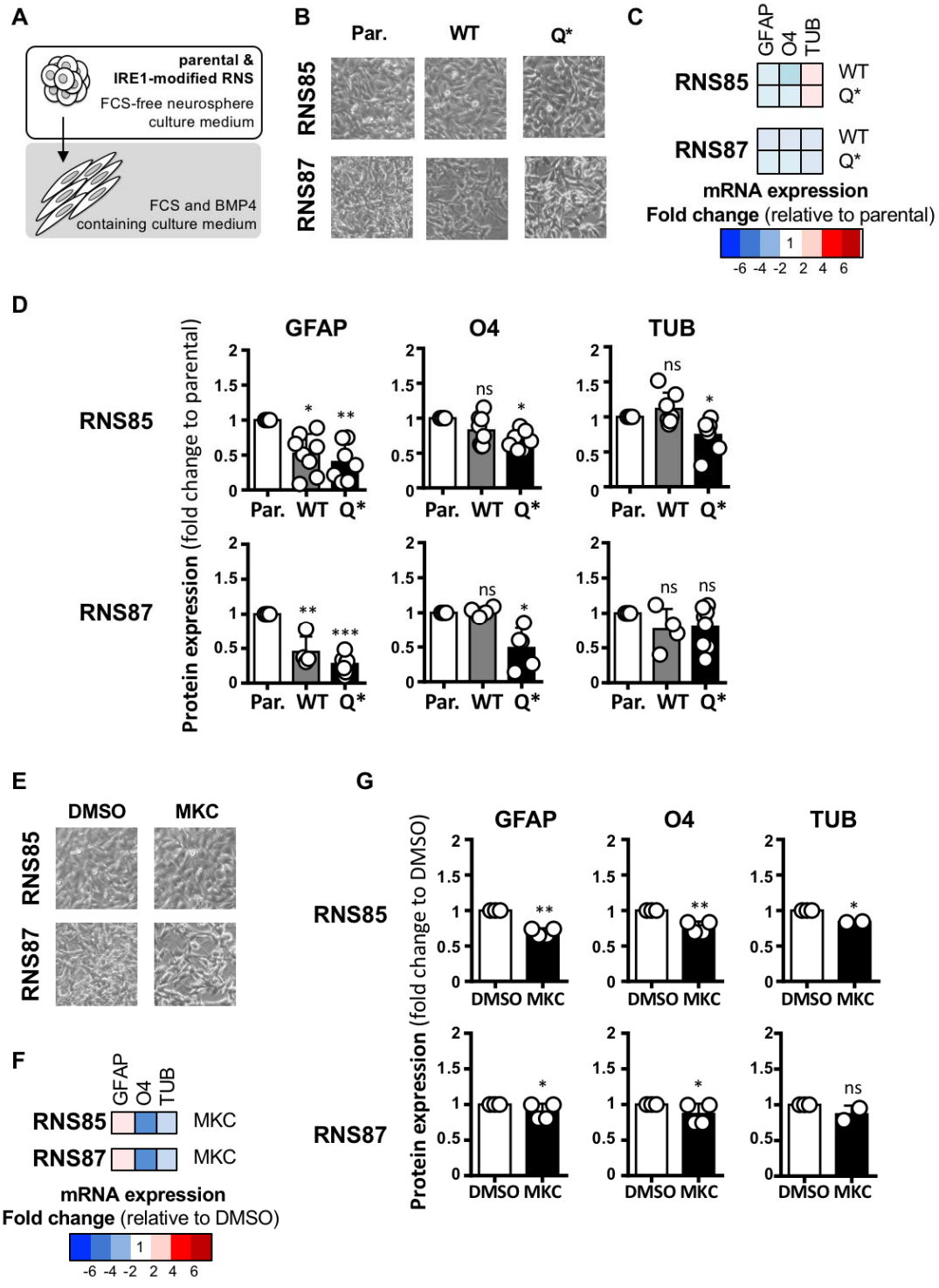

FIGURE 5

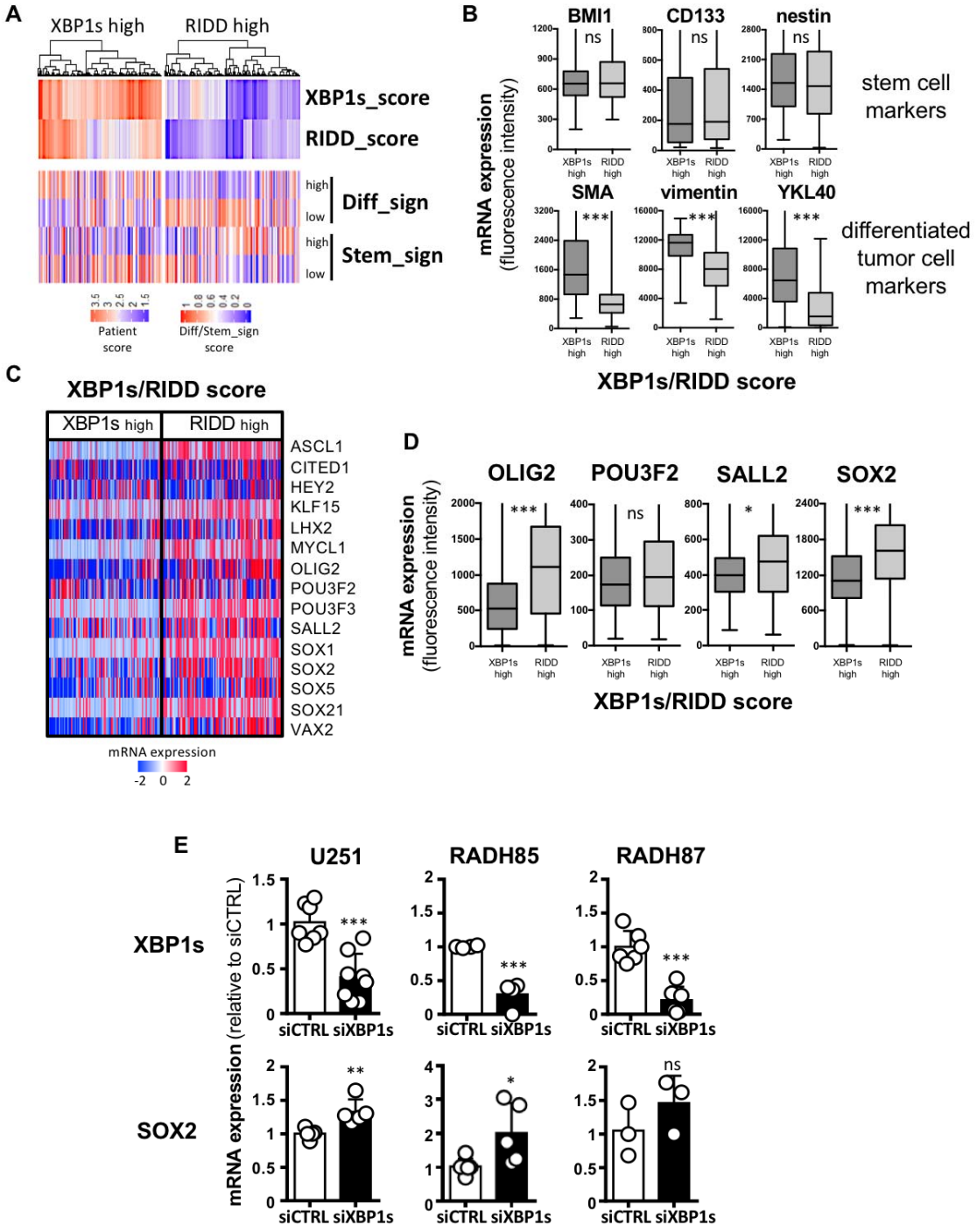

FIGURE 6

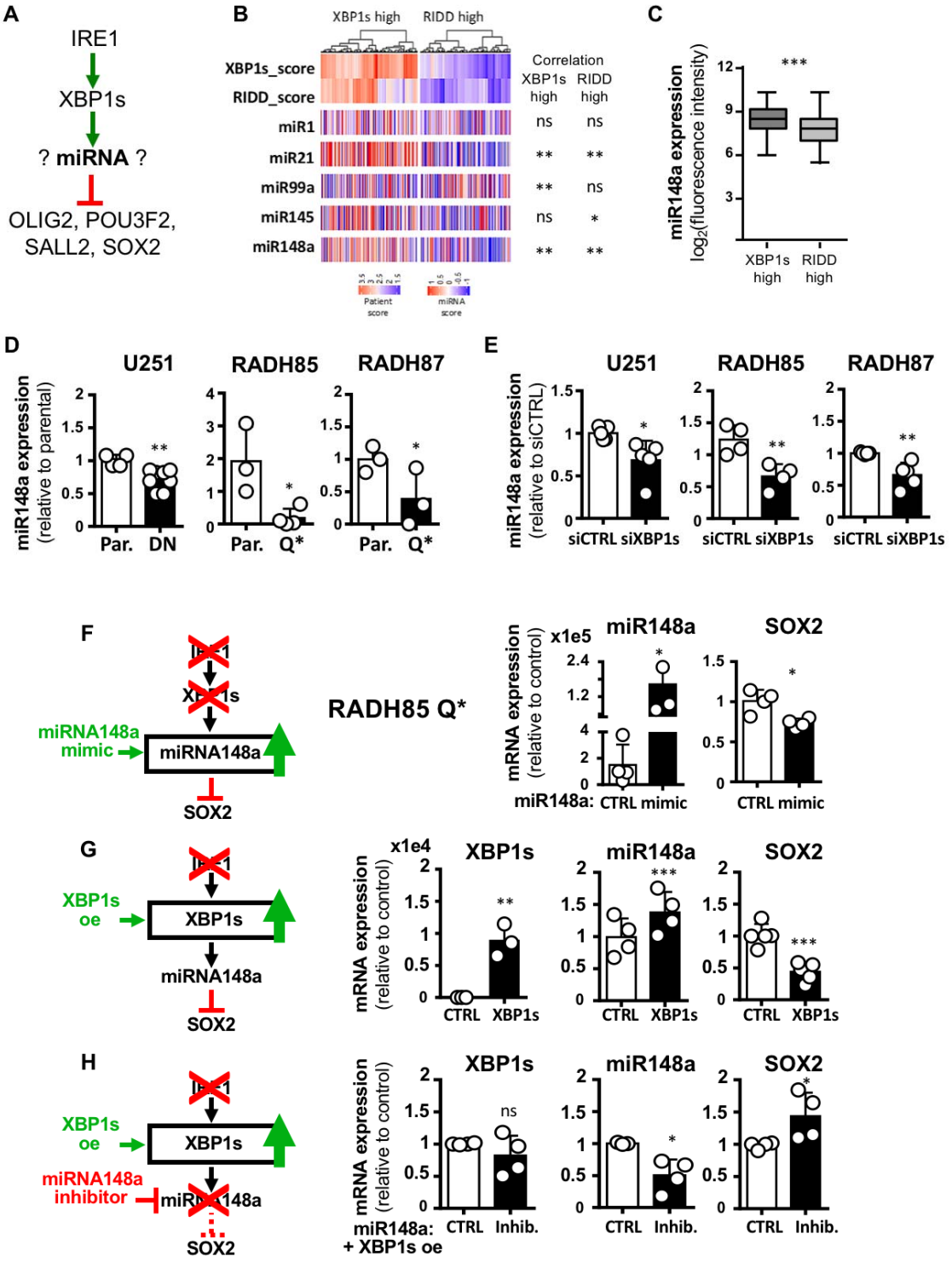

FIGURE 7